

Incremental explosive analysis and its application to performance-based assessment of stiffened and unstiffened plates

Masoud Biglarkhani¹, Keyvan Sadeghi^{2,*}

¹*Civil Engineering Department, University of Hormozgan, Bandar Abbas 3995, Iran.*

²*Mechanical Engineering Department, Buein Zahrah Technical University, Qazvin 3451745346, Iran.*

Received: 29 July. 2017, Accepted: 25 Sep. 2017

Abstract

In this paper, the dynamic behavior of square plates with various thicknesses and stiffening configurations subjected to underwater explosion (UNDEX) are evaluated through a relatively novel approach which is called Incremental Explosive Analysis (IEA). The IEA estimates the different limit-states and deterministic assessment of plates' behavior, considering uncertainty of loading conditions and dynamic nature of explosive loading. In this new approach, intensity parameter of explosive loading is enhanced in an incremental manner and response of the target plate is recorded for every depth-stand-off loading condition. Then, the multi IEA curves are derived from several simulation results. The fractiles method is employed to summarize large amount of IEA curves' data in a predictive mode. In addition, some summarized damage probability indicators such as fragility curves are extracted that provide useful information for quantitative damage analysis of plates in UNDEX loading. Results show that the IEA is a promising method for performance-based assessment of marine structures subjected to UNDEX loading.

Keywords: Air-backed plate; Underwater explosion (UNDEX); Depth parameter; Stand-off distance; Incremental explosive analysis (IEA); Intensity parameter; Fragility; Uncertainty

* Corresponding author: keyvan.sadeghi@bzte.ac.ir

1. Introduction

Air-backed plane plates are common structural components in marine structures. Dynamic response analysis of plate panels subjected to UNDEX is complex due to various parameters such as fluid-structure interaction, high strain rates, large deformation, material nonlinearity as well as complexities associated with UNDEX loading itself. Experimental studies play an important role in understanding the structural behavior of hull panels of marine structures subjected to UNDEX. However, UNDEX experiments are very expensive and tests are generally limited to scale down specimens and limitations in variation of involved parameters. Although full scale tests are conducted in some countries, their data are rarely published. On the other hand, numerical simulations have been applied successfully to analyze the dynamic response of submerged structures under shock loading. Numerical procedures, if implemented correctly, can be very efficient for studying UNDEX problems, where involved parameters must be varied in an extended range. Research concerned with response of structures subjected to UNDEX is numerous. Both experimental and numerical methods are implemented. As can be expected analytical methods have several limitations to be applied to UNDEX problems due to the complexities of the problem. Cole [1] reports that the earliest experimental work on the explosive loading of an air-backed plate or diaphragm was done by Modugno in 1919. Ramajeyathilagam [2] studied nonlinear response of steel rectangular air-backed plates subjected to underwater explosion using experimental and numerical methods. They used MARC finite element code for predicting structural response of plates and applied the shock loading based on a simplified model. H. Gharababaei et al. [3] obtained the deformation profile of circular plates with distinct materials facing blast loading in order to better perceive the effects of some important parameters on central deflection and overall form of the deformed plates both analytically and experimentally. Moharami et al. [4] investigated the effect of underwater explosion loading on the two semi elliptical surface cracks in the pressurized pipelines and derived the dynamic stress intensity factors for the internal and external cracks. Rajendran [5] performed experiments on rectangular plates and proposed some empirical formulae that can be used to predict the plate's permanent deflection. In another work Rajendran and Narasimhan [6] studied the response of circular and rectangular plates under UNDEX loading. In their work, a microscopic electron scanning was used that shows micro void creation, which is a fracture mechanism that may happen in plates. Hung et al. [7] studied the elastic dynamic response of aluminum rectangular plates subjected to UNDEX by experimental and numerical methods. The USA/DYNA code was implemented in modeling of the problems and a good agreement between tests and numerical results were observed. The correlation between numerical and experimental results

was weaker for near distant stand-offs. Gupta et al. [8] studied the tearing and deformation behavior of the weld box and high strength steel plates subjected to UNDEX by using numerical simulations in ABAQUS/Explicit environment. Both simple and stiffened plates were considered. Li and Jiang [9] introduced an efficient approximate method for prediction of permanent deformation of plates subjected to UNDEX without modeling of the surrounding medium and reduced the computational costs significantly. Rajendran [10] investigated UNDEX loaded plates in linear elastic domain using numerical simulation in LS-DYNA. The same author [11] studied the reloading effect of remote underwater explosion on the plane plates and a comparison between theoretical and experimental results has been made. In a different work, Ren and Zhang [12] did a combined experimental and numerical research to analyze the deformation and failure characteristics of aluminum alloy plates. In their work, shock waves were produced by non-explosive means. They used a gas tube to induce high velocity impact on a piston accommodated in a cylinder-shape duct to simulate explosive loading on circular aluminum plates. There are also a lot of experimental and theoretical research concerned with air blast loaded plates [13] and some of their primary results were implemented in underwater explosion cases. Nevertheless, some corrections and modifications must be applied on them before using in UNDEX problems. Complicated nature of UNDEX phenomenon by its own has attracted attention of some researchers to investigate pure underwater explosion event and its bubble consequences. For example, Yeom [14] investigated underwater explosion phenomenon in a more basic and fundamental approach. He used a very complicated model to take into account all of the process factors. He analyzed all the essential aspects of the UNDEX such as shockwave propagation through the medium, the interaction of the shock waves and pulse waves with different boundaries and free surface of the medium and water jetting effect of diminishing gas bubble near the surface of a structure. Also, Grujicic et al. [15], in a computational study used AUTODYN as a hydro-code to investigate the mitigation mechanisms of underwater explosion bubbles. Wang et al. [16] in a detailed numerical study investigated the effect of UNDEX shock and its propagation where boundaries are near to the explosive charge. To the best knowledge of authors there is no research which has investigated the effect of combination of depth and stand-off factors on response of plates subjected to UNDEX. Most of research concerning this subject are confined to a fixed stand-off distance and the variation of depth parameter is neglected in most of studies. Changing the depth parameter is more challenging than the stand-off distance because it requires substantially deeper UNDEX testing pools which are not available in most conventional test centers. Furthermore, direct simulation of depth effect on UNDEX loading is an expensive and tedious task because it requires

modeling of the whole water above the level of test point. This problem can be overcome indirectly by simulation of depth parameter effect via average hydrostatic pressure of surrounding medium. Countless combinations of depth and stand-off distance pairs can be considered as the plate UNDEX loading conditions. To be practical and to cover a wide spectrum of loading conditions in an effective way an incremental loading procedure can be applied. Therefore, this study aims to develop a relatively novel approach which is able to overcome the above-mentioned shortages that are not covered in the previous studies. It is called the Incremental Explosive Analysis (IEA), which can be a reliable method of predicting structures' behavior from elastic range to yielding and finally collapse of the system. The IEA can be employed in the design and/or assessment of marine structures subjected to UNDEX loading. In fact, it can evaluate different performance levels or limit-states and ultimate capacity of structures by using nonlinear dynamic explosive analyses. A relatively similar concept called Incremental Dynamic analysis (IDA) has been established in recent years by Vamvatsikos and Cornell [17, 18] in order to assess performance of the building structures subjected to seismic loading such as earthquake. Further details about this method can be found in related literature [19]. The use of this method is investigated by many researchers on different type of structures such as building [20], dams [21] and bridge I. [22]. Other researchers introduced novel approaches based on the IDA method and studied the seismic performance of offshore jacket-type structures [23-25]. They reported that their presented model yields reasonable accuracy and little computation effort. Based on the IDA, relatively novel methodologies have been proposed by some researchers for environmental loads other than earthquake, such as Incremental Wave Analysis (IWA) [26], Endurance Wave Analysis (EWA) [27] and Incremental Wind Wave Analysis (IWWA) [28]. Furthermore, similar methods have been implemented to evaluate the performance of a structure under similar loading conditions. For example, R.A. Izadifard et al. [29] adopted a displacement-based methodology to investigate the performance of a steel plate under blast loading using AUTODYN.

In the present study, the IEA is proposed as a new methodology to study the submerged air-baked plates under UNDEX loading in a whole range of elastic and elasto-plastic deformation spectrum. In this approach, by using various combinations of major factors in UNDEX, such as charge depth and stand-off distance, the loading intensity is enhanced in an even (equaled) paced of increments. The inverse of scaled distance is chosen as the intensity measure (IM) and the maximum of deflection time history and the effective strain of plates are chosen as damage measures (DM). Numerical simulations are performed in AUTODYN hydro-code environment and rigorous coupled Eulerian-Lagrangian

models are implemented for this purpose. Then, the multi IEA curves are derived from analysis which is representing the plates' responses. Three distinct limit-states are considered based on the reliable references which are discussed in the next section. In order to summarize the extracted IEA curves, the cross-sectional fractiles method is employed as a large amount of data is gathered. This will reduce the data to the distribution of DM given IM and to the probability of exceeding defined limit-states given the IM level. In addition, the fragility curves are derived to acquire a design tool for similar situations with uncertainty in loading conditions. The IEA is implemented on four configurations of stiffened and unstiffened square plates under different loading conditions. The output of the analysis provides useful data about the structural performance of plates under simulated loading conditions.

2. Incremental Explosive Analysis

2.1 New aspects of IEA

The capability of capacity prediction of marine structures subjected to UNDEX loading and gaining intuition of the structural behavior, led to a demand for innovation in the design of this type of structures. In UNDEX, the entire range of structures' behavior, from elastic to inelastic and finally collapse of the system, and deterministic assessment of structural performance is an important challenge for designers. UNDEX's effect on plate structures may appear as a simple problem at first glance but innate complicacy of UNDEX loading itself makes this problem an involving task. Altering parameters of UNDEX loading which in this study are depth and stand-off factors, can drastically change the spatiotemporal distribution of loading. These changes are severely nonlinear and any attempt to find a concise relation covering all possible situations is an abortive task. Although there are numerous semi-empirical relations offered by researchers in this realm to anticipate the structural response of plates subjected to UNDEX loading; often an inherent error will remain particularly in cases which condition of problem deviated from what was assessed for extraction of formula. Numerical models if implemented by being cognizant about their meticulous aspects can be a good solution to overcome this problem. However, results extracted from single simulations do not offer adequate data to decide about the design of structure. This issue previously was a challenge for structural engineers who engaged in design and analyze of structures subjected to earthquake seismic loads. As can be expected, there are uncountable loading conditions which can be created by combination of depth and stand-off factors. Evaluation of response of plates subjected to numerous loading conditions is not an easy task and also is not imperative. Hence, a limited number of loading conditions will be investigated by varying both the depth and stand-off distance parameters to extract adequate level of information. Stand-off distance parameter after a particular distance has less

significant effect on the distribution of loading pressure on the plate due to the more uniform effect of overpressure on the target. By enhancing the stand-off parameter, the distribution of explosion overpressure on the surface of object will converge to a more homogenous pressure profile. This distance depends on the size of target. Therefore, the maximum of the stand-off distance is determined in such a way that the whole plate surface experiences a homogenous pressure distribution. But the depth parameter can be altered in a wider domain. This domain may be extended to cover its effect on more rigid structures such as stiffened ones. However, by considering characteristic of aforementioned loading parameter of UNDEX and its effects on structures, the relatively novel approach called Incremental Explosive Analysis (IEA) is introduced. The IEA involves performing multiple nonlinear dynamic analyses of a structural model of plates under several levels of explosive intensity. The scaling levels are appropriately selected to force the plate structure through entire range of its behavior. Then, appropriate post-processing can generate the results in term of IEA curves, one for each loading condition which is here combination of stand-off distance and depth parameter, of the explosive intensity, typically represented by a scalar intensity measure (IM), versus the structural response or demand. The structural response is identified as damage measure (DM) and can be any structural response quantity that relates to structural damage. This method also enables checking for multiple performance levels or limit-states. The most objectives of this method include the followings: (1) thorough understanding of the range of response or “demand” versus range of potential levels of an explosive intensity, (2) better understanding of the changes in the nature of the structural response as the intensity of explosive charge increases, (3) better understanding of the structural implications of rarer/more sever explosive intensity levels, (4) the estimation of structural dynamic capacity, (5) finally, generation of multi IEA curves indicating how variable (or stable) all these items are from explosive intensity level to another. By implementing the proposed method, an integrated approach for quantifying the effect of every loading condition will be possible and designers will have a broader vision for assessment of design process by being informed about the probability of every drastic condition occurrence and this will lead to an optimized design eventually. However, the numerical analysis required to evaluate the structure response under different conditions are very time consuming and having a more detailed model would increase the analysis time significantly.

2.2 Implementation of IEA procedure

Several steps are required for applying IEA in order to determine the performance of a structure: i.e. (1) to form a proper nonlinear structural model, (2) choosing suitable intensity measures (IM) and representative damage measurers

(DM), (3) selection of scaling levels corresponding to IM, (4) applying proper interpolation, (5) estimation of the probability distribution of the structural demand given the explosive intensity by summarization techniques, (6) definition of performance levels or limit-states to calculate the corresponding capacities. Thus, in order to perform the IEA on a structure, at first, it is essential to define an intensity factor as a representative of the intensity of applied loading condition. The scaled distance is a well-known empirical parameter that can be chosen as a basis for the definition of intensity factor. According to Cole [1], it can be defined as follows:

$$Z = \frac{R}{\sqrt[3]{W}} \quad (1)$$

where W is the equivalent TNT mass of charge in kg and R is stand-off distance in meter measured from the center of spherical charge to the location of gauge point. In this study, the inverse of the scaled distance is chosen as the intensity measurement parameter:

$$IM = \frac{1}{Z} = \frac{\sqrt[3]{W}}{R} \quad (2)$$

The standoff distance between the explosive and the structure and depth of the explosion are two other dominant factors in UNDEX loading. The major effects of the depth parameter is related to the temporal variation of pressure, duration of UNDEX pulsations and bubble migration [6]. Another important effect of the depth parameter is concerned with the preloading of the structure due to initial hydrostatic pressure. To better quantify this effect, a scaled depth parameter is implemented as follows [30]:

$$\beta = \frac{h}{\sqrt[3]{W}} \quad (3)$$

where W is the equivalent TNT mass in kg and h is depth in meter measured from the water surface. Therefore, nine combinations of the probable loading conditions are considered here to take into account a wide range of possibilities. Table 1 represents the implemented (SD, β) loading conditions.

Table 1 Combination of various Stand-off distance (SD) and depth parameters (β)

SD	β
700	7
1400	40
2100	90

Since the stand-off distance were chosen far enough to have the homogenous pressure distribution on the plate surface and no drastic interactions between the structure surface and bubble gasses were involved, then the inverse of the scaled distance can be used as intensity measurement value. In the IEA, the IM values will be increased incrementally so that the whole spectrum of the structural response will be covered i.e. from elastic to elasto-plastic and to the final collapse. It should be mentioned that an individual nonlinear numerical analysis is conducted for obtaining the structural response for every IM value for all nine combinations (SD, β).

After an accurate definition of IM, it is required to define the damage measurement (DM) parameter to indicate the structural response under distinct loading conditions and IMs. In this study, two different damage parameters are considered. First, the ratio between maximum plate deflection at the middle region to the plate half length (θ_{max}), or the maximum rotation of the plate edge. This parameter was selected here in the present study as the index of the plate response since it is known as one of the simplest quantities to be measured as the response of the plate structures. In addition, it has been extensively utilized in the previous researches and even creditable standards such as UFC-3-340-02 [31] suggests this parameter. Second, the ductility ratio which is defined as:

$$\mu = \frac{\varepsilon_M}{\varepsilon_{El}} \quad (4)$$

where ε_M and ε_{El} are the equivalent strain in plate center and the maximum elastic strain, respectively. Then, the IEA curves can be generated and pinned on the $IM - DM$ plane for every combination of (SD, β) representing the structural responses for the different explosive masses and environmental factors. After extraction of the desired IM and DM values from each of the dynamic analysis, a set of discrete points are available for each combination of (SD, β) that reside in the $IM-DM$ plane and lie on its IEA curve, as in Fig. 1. By interpolating them, the entire IEA curve can be approximated and no need to perform additional analyses. To do this, a realistic interpolation such as a basic piecewise linear approximation, or the superior spline interpolation needs to be generated in order to accurately represents the real IEA curves. Hence, in this study, the spline interpolation is selected as shown in Fig. 1 [32, 33].

In order to assess the performance of the plates under different UNDEX conditions, it is essential to establish and define limit states on the IEA curves. Therefore, it was decided to use three different criteria based on the critical situations of the plates under loading. These are the elastic limit-state

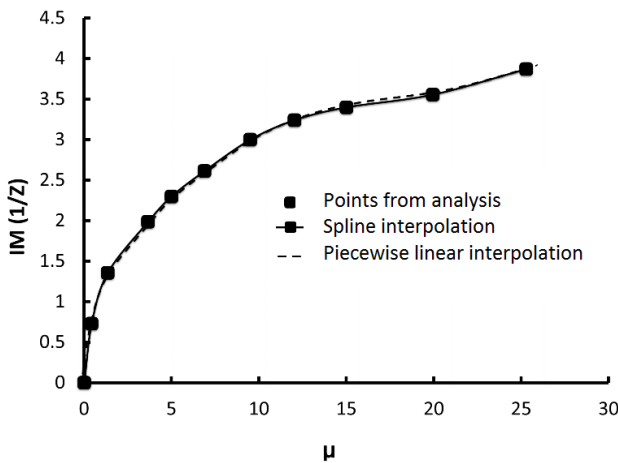


Fig. 1 Obtained IM-DM points for (700,7) for different IM values, using spline and a piecewise linear approximation

which relates to stable condition of the structure (Elastic), the incipient of total failure (LS-2) and the mid-term limit-state (LS-1) between the elastic-state and final collapse. The corresponding DM values for these three different limit states are defined according to UFC-3-340-02 [31] and provided in the section 6.

IEA simulations that generate the curves and subsequently defining the limit-state capacities will gather considerable amount of data. Presentation of these data in multiple curve diagrams may be useful for a brief comparison of the effect of various parameters and display a wide range of behavior; however, they cannot be handled easily by a designer. Furthermore, plate response distributions for different levels of IM are not similar. Thus, to address this issue, appropriate summarization technique is employed in order to reduce this data which provide indirect information about probability of occurrence of an identical level of DM for every IM. In this study, the cross-sectional fractiles method is implemented for IEA curves summarization [18] and the capacities of the limit-states are summarized into mean value and difference between two fractiles. To do so, the 16%, 50% and 84% fractile values of DM ($DM_{16\%}^C, DM_{50\%}^C, \text{ and } DM_{84\%}^C$, respectively) and IM ($IM_{16\%}^C, IM_{50\%}^C, \text{ and } IM_{84\%}^C$, respectively) for each limit-state are chosen to be calculated accordingly. More details about this method are discussed in section 6.

The above-mentioned characteristic can be more illustrative in fragility curves, where the probability of occurrence of various limit states can be extracted for every IM level. Most of blast resistive structures are designed to tolerate extreme loading conditions where the probability of occurrence of these loadings is not similar to the relevant threats and often high safety-factors are used in design. This can be a problem for sea going objects where weight optimization is crucial for efficient fuel consumption. In this regard, IEA curves can be a design tool for efficient design of stiffened plates in explosion resistive marine structures.

3. Numerical modeling

The effect of underwater explosion on structures is associated with many complicated nonlinear phenomena, rooted in interaction of solid boundary and inertial medium of water. Moreover, very high rated loading due to explosive loading, strain rate effects on material behavior and large deformations can enrich this list. Considering these complexities the application of analytical methods will be limited to the simplified solutions to obtain rough estimates [34, 35]. For precise design and analysis, reduced scale experimental methods are very useful. Nevertheless, most of the full scale tests are conducted under military programs and their data are classified. Another effective and powerful method, if implemented correctly, is numerical simulation.

Coupled numerical models if are set up by correct procedures can predict complicated FSI problems in a feasible way. In UNDEX loading the deformation of fluid medium is very high in comparison with solid continua and this fact must be taken into account in modeling FSI problems. Eulerian approach is used to discretize the water medium and ordinary nonlinear shell Lagrangian method is utilized to avoid numerical troubles arisen from sever distortion of elements. Shell elements are in full coupling with surrounding fluid. Explosion must be modeled from the beginning of detonation to capture shock wave distribution in water effectively. As discussed earlier, since the underwater explosion phenomenon has a considerable level of nonlinearity especially in near distance charges a fully detailed numerical approach is utilized for analysis.

3.1 Governing FSI equations

Numerous sources are available for the detail of finite element and computational fluid dynamics associated with FSI problems and the coupled Eulerian-Lagrangian procedure. The discretized differential equations of motion can be presented as follow [16]:

$$M\ddot{x} + C\dot{x} + Kx = F(t) \quad (5)$$

where x is the structural displacement vector and M , C and K are structural mass, damping and stiffness matrixes, respectively. The parameter $F(t)$ is the force vector which is calculated according to FSI algorithm. Superimposing imaginary fluid mesh on the interface of fluid and solid leads to compatibility relations of submerged structure:

$$F(t) = -GA_f(p_i + p_s) \quad (6)$$

Where p_i is the incident pressure of fluid (here UNDEX overpressure and pulsations), p_s is the scattered pressure of the structure, G is a matrix that couples structural degrees of freedom to the fluid grid and A_f is the matrix that stores information of areas of Lagrangian elements in fluid cells. The compatibility equation that enforces the fluid and structure surface grids to have the same normal velocity may be expressed as follows:

$$G^T \dot{x} = \mu_i + \mu_s$$

in which superscript T refers to matrix transposition, μ_i is the incident water particle velocity from the UNDEX and μ_s is scattered water particle velocity induced from structural interaction.

3.2 JWL equation of state

The high explosives detonative reaction associated with high amount of chemical energy conversion to heat and mechanical waves is a very complicated process and the molecular reaction cannot be exactly modelled by a continuum model. However, the process of energy conversion can be predicted with an

acceptable accuracy by definition of an equation of state (EoS) such as Jones, Wilkins and Lee (JWL) equation which models the pressure generated by chemical energy in an explosion as follows:

$$P = C_1 \left(1 - \frac{\omega}{R_1 \nu}\right) e^{-R_1 \nu} + C_2 \left(1 - \frac{\omega}{R_2 \nu}\right) e^{-R_2 \nu} + \frac{\omega E}{\nu} \quad (8)$$

where ν is the specific volume of detonation products over the specific volume of undetonated explosive, E is the specific internal energy and C_1 , C_2 , R_1 , R_2 , ω are material constants. These coefficients are available from experiments and for TNT as a standard and relevant high explosive material they are given in the Table 2 [36]

Table 2 JWL constants of TNT

C_1 (GPa)	C_2 (GPa)	R_1	R_2	ω	ρ_0 (kg/m ³)
373.7	3.74	4.15	0.9	0.35	1630

3.3 EoS of water

Water as an incompressible fluid has negligible strength and its dynamic behavior can be modeled with adequate accuracy using definition of a polynomial equation of state (EoS). This EoS defines the pressure as:

$$p = A_1 \mu_d + A_2 \mu_d^2 + A_3 \mu_d^3 + (B_0 + B_1 \mu_d) \rho_0 e \quad (9)$$

for $\mu_d > 0$ (Compression)

$$p = T_1 \mu_d + T_2 \mu_d^2 + B_0 \rho_0 e \quad (10)$$

for $\mu_d < 0$ (Tensile)

where $\mu_d = \frac{\rho}{\rho_0} - 1$ and ρ_0 is the initial density,

A_1 , A_2 , A_3 , B_0 , B_1 , T_1 and T_2 are constants that are presented in Table 3 [36] and e is the internal energy per unit mass. The effect of depth can be accommodated in the water internal energy using the following relation:

$$e = \frac{\rho g h + p_0}{\rho B_0} \quad (11)$$

where ρ is the density, h is the depth measured from the free surface of water, p_0 is the atmospheric pressure and g is the gravitational acceleration (9.81 m/s²).

Table 3 Polynomial EoS for Water

A1 (GPa)	A2 (GPa)	A3 (GPa)	B0	B1	T1 (GPa)	T2 (GPa)	ρ_0 (kg/m ³)
2.2	9.54	14.57	0.28	0.28	2.2	0	999

3.4 EoS of Air

In this study, plates are considered to be air backed; therefore, an equation of state (EoS) for modeling of air effect is needed. Typically ideal gas EoS is sufficient for accurate

results. This is defined by the ideal-gas gamma-law relation as:

$$p = (\gamma - 1) \frac{\rho}{\rho_0} E \quad (12)$$

where E is the specific energy, γ is the ratio of constant pressure over constant volume specific heat (=1.4 for air), ρ_0 is initial density (=1.225 × 10⁻³ g/cm³) and ρ is current density. If standard air condition is specified, E must be set to 253.4 (kJ/m³).

3.5 Johnson-Cook Strength Model for Steel

Usually metals exhibit a strain rate sensitive behavior when subjected to high rate dynamic loading. Steel as the main material for construction of marine structures has considerable sensitivity in comparison with other metals. In most UNDEX loadings, strain rate can reach to 10⁴/s hence for accurate results an acceptable rate sensitive strength model must be used. The Johnson-cook model can predict changes in yield stress of metals and in particular steels accurately. The 4340 Steel has potential for being utilized in marine and submarine structures. The Johnson-cook model relates the flow stress to the strain, strain rate and temperature as follows [36]:

$$\sigma_y = (A + B\varepsilon_p^n)(1 + C \log \dot{\varepsilon}_p^*) (1 - T_H^m) \quad (13)$$

where σ_y is flow stress, ε_p is normalized plastic strain, $\dot{\varepsilon}_p^*$ is normalized plastic strain rate and T_H^m is the homogenized temperature which is defined by the following relation:

$$T_H^m = \frac{T - T_r}{T_m - T_r} \quad (14)$$

where T_r is room temperature and T_m is melting temperature of the material. The coefficients A , B , C , n and m in Eq. (13) are material constants which are specified for 4340 steel in Table 4 [36]

Table 4 Johnson-Cook properties of 4340 steel

A (MPa)	B (MPa)	C	n	m	T _m (°K)
792	510	0.014	0.26	1.03	1793

4. Validity of implemented numerical scheme

As mentioned earlier, the validity of numerical simulations must be checked in every study and this can be performed in best way if the results of numerical model are compared with those of experiments. The available experimental data do not necessarily match with the numerical case studies. Most of the published UNDEX related experimental data are confined to scale down tests conducted on small structures and may not be used directly in real marine or submarine structures. Size of plates in the present work is in the full scale and to the best

knowledge of authors, there is no published results conducted in this scale. Hence, valid experimental research results are chosen for the purpose of comparisons and validity study. In an extended experimental and numerical study, Ramajeyathilagam et al. [2] investigated the response of steel plates subjected to underwater blast loading. They carried out tests on two types of mild (MS) and Hard (HS) steels and compared their numerical result, simulated in MARC code, with experimental ones. Due to vicissitudes in using TNT in underwater tests, PEK is implemented in [2] PEK has an equivalent mass 1.17 times of TNT, so mass of PEK charges must be multiplied in 1.17 to find TNT equivalent mass. To make a comparison of experimental data of [2] with the selected numerical scheme of the present study, a full model is set up in AUTODYN environment which contain surrounding water and structure. This model is explained in [2]. HS specimens in [2] have 0.3 × 0.25 m² exposed area and due to symmetry only one quarter of model is needed for numerical simulation. The thickness of specimens is 4 mm and they are fabricated from a type of steel with 400 MPa yield stress. The Johnson-Cook equivalent coefficients of this steel are given in Table 5. Water medium is discretized by using 11250 regular cubic Eulerian cells and 225 shell elements are used for construction of one quarter model of plate. The stand-off distance for explosive charges is set to 15 cm against target plates. All edges of plates are assumed to be perfectly clamped and transmit boundary conditions are applied on all of outer planes of Eulerian model to simulate a semi definite medium without any wave reflection. For better understanding of detonation phenomenon, remapping ability of AUTODYN is used. In remap process, the explosion of high explosive material is modeled in 1-D wedge environment and after the shock wave's front reaches the plate vicinity, results of one dimensional simulation are mapped onto a 3-D model. This capability of AUTODYN can significantly help to achieve highly accurate results where may not possible in 3-D model due to tremendous numerical cost. Fig. 2 illustrates a schematic of 3-D model after remapping process. Experiments in [2] are classified by introducing a shock factor that is defined as follows:

$$SF = 0.45 \times \frac{\sqrt{W}}{R} \quad (15)$$

where W is mass in kg of equivalent TNT for high explosive material and R is the stand-off distance in meters measured from center of plate to standing point of explosive charge. Stand-off distance in [2] is set to 15 cm in order to achieve permanent deformation. Results of the present study using hydro-code simulation and those of [2] are presented in Table 6 for comparison.

There is very good agreement between hydro-code calculations and experimental results showing that the employed procedure can be a reliable tool for anticipation of UNDEX loading on shell structures.

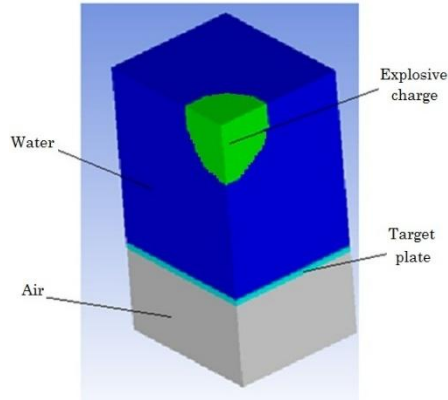


Fig. 2 Three dimensional model of problem in [2] reconstructed in AUTODYN

Table 5 Johnson-Cook constants of HS steel used in [2]

A (MPa)	B (MPa)	C	n	M	T _m (°K)
400	250	0.27	0.98	1.03	1793

Table 6 Results of experiment and hydro-code simulation. Central permanent deformation

8	R (m)	W (g)	shock factor	Experiment [2] (mm)	Present Simulation (mm)
			$(0.45 \frac{\sqrt{kg}}{m})$		
HS7	0.15	5	0.212	12	10.9
HS8	0.15	10	0.3	23	22.6
HS9	0.15	20	0.424	32	31.5
HS10	0.15	50	0.671	59	57
HS11	0.15	70	0.794	72	71

5. Problem Description

5.1 Geometry of target plates

In this paper four different plate configurations are studied. The plate configurations are summarized in Fig. 3. Plate dimensions are 3*3 m. There are two simple plates with two different thicknesses: 10 mm and 18 mm, and two stiffened

plates with stiffeners in one-direction and in orthogonal directions parallel to plate edges (cross directions).

The Stiffener thickness is set to 10 mm and their height is 100 mm .They are applied on plates in an equidistant manner. As mentioned earlier it is assumed that plates are fabricated from 4340 Steel.

5.2 Numerical Assessment of Problem

General scheme for numerical modeling of UNDEX loading on target plates is similar to which is described in Section 4. Here further detail specifications which are implemented are discussed. For every specific stand-off distance a distinct Eulerian grid is utilized for discretization due to different distances from center of explosive charge to center of plates. These Eulerian grids are fixed for all of plates’ configurations. There are 36000 (90*20*20), 50000 (125*20*20) and 80000 (200*20*20) Eulerian cells used for near (700 mm), medium (1400 mm) and far (2100 mm) stand-off distances respectively, while 900 (30*30) Lagrangian shell elements was implemented in construction of base plate models and 120 (30*4) elements for stiffener pieces.

Meanwhile validity analysis shows that regular distribution of Eulerian grid is adequate for most of remote UNDEX problems however in very puissant UNDEX cases very large deformations may be probable and finer concentrated grid is used in vicinity of plates for better capturing of very large deflections and sever pressure gradients. The convergence of response of the system due to Eulerian mesh refinement is observed and presented in Fig. 4. Fig. 5 illustrates a caption from aforementioned Eulerian grids. It should be noticed that the computational effort for evaluation of Eulerian grid is generally much higher than Lagrangian approach. Therefore, a compromise between accuracy and computation time must be performed. Hence, the same configuration used in the verification section was also utilized here to obtain acceptable results. Moreover, most of the fluid medium surrounding the plate has negligible effect on the final response of the plates.

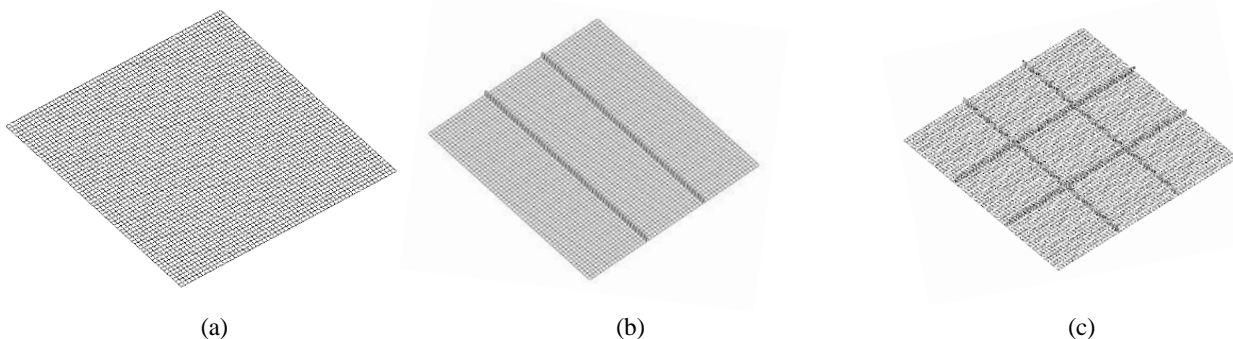


Fig. 3 Plates geometrical presentation; (a) simple, (b) one directional and (c) cross directional stiffened plates

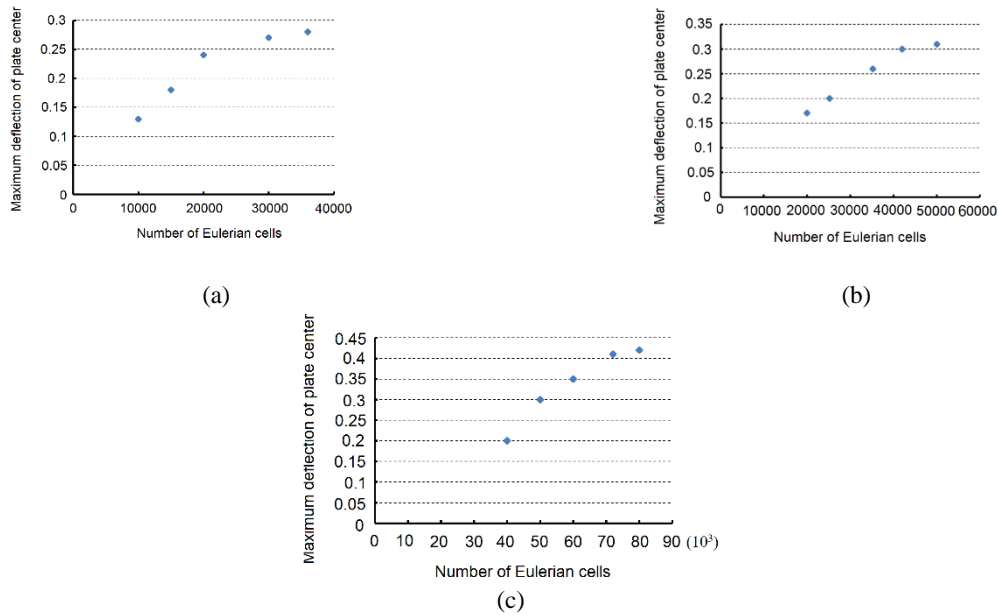


Fig. 4 Numerical convergence according for various stand-offs, (a) 700 mm stand-off-1/Z=2, (b) 1400 mm stand-off-1/Z=1.5 and (c) 2100 mm stand-off-1/Z=1.

For every increment, required mass of explosive is calculated and according to depth parameter, internal energy of water is evaluated by means of Eq. (11). By applying these conditions on 1-D numerical model and performing simulation up to the moment which shock front reaches to vicinity of plate, results are mapped onto 3-D one-quarter model where mapping origin is coincident with origin of 3-D model. Fig. 6 depicts a schematic of IEA process implemented in the present study.

Then, extensive simulations with the incremental *IMs* provided in Table 7 are performed and the corresponding *DMs* are pinned to the *IM – DM* plane and build the one-line IEA curve. Finally, for a specific configuration i.e. one and cross directional stiffened plates, the IEA curves are obtained. These sequences are performed on the all four different configurations with corresponding incremental values of *IMs*.

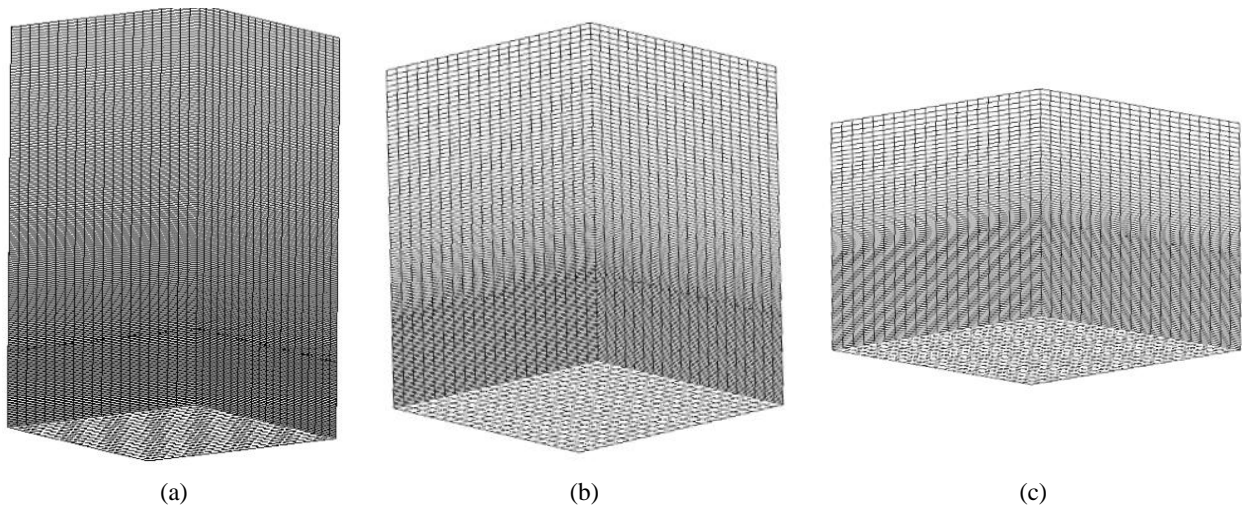


Fig. 5 Eulerian grid for discretization of surrounding water medium; (a) far, (b) medium and (c) near stand-off explosions

6. Results and discussion

By applying the method described in the previous sections,

numerical simulations are carried out and corresponding results are presented in this section. Fig. 7 illustrates nine pressure histories as sample Intensity Measures (*IM*) and

shows the tangible differences between them. Empirical research of Li [9] uncovered that a nearly linear relation exists in unbounded domains between the $\frac{1}{Z}$ and the overpressure of UNDEX, that can be stated as:

$$P_{\max} = 52.4 \left(\frac{1}{Z} \right)^{1.13} \quad (16)$$

The first pressure peak indicates the very beginning of shock wave effect which induces maximum pressure on the structure or plate followed by several pulsations regarding to the bubble cyclic expansion and contraction effects and as well as pressure reflections from target. Due to damping of water, these bubble oscillations dissipated and will have less detrimental effect after two or three pulsations. Fig. 8 depicts deformed configuration of plates when the maximum Damage Measure (DM) happened. It should be mentioned that the maximum point of DM time history is recorded for constructing IEA individual curves.

According to section 2.2 and as discussed in [17] analogous to the stability of steel structural frames, when structure undergoes stresses (or strains) beyond the elastic range of material, the elasto-plastic condition is met in the structure but, as suggested by UFC-3-340-02 [31], the maximum rotation of plate edge, θ_{\max} , shall not exceed 12° ($\theta_{\max} < 12^\circ$). This limit

state is called LS-2 which is the incipient of total failure of the structure.

According to these definitions and UFC-3-340-02 [31], the value of corresponding ductility ratio for the LS-2 becomes 20 ($\mu = 20$). Moreover, again offered by UFC-3-340-02 [31], the structure is stable and safe when the ductility ratio do not exceed 10 ($\mu = 10$), which is called the LS-1 in present study.

For normalized high strength steel 4340, the maximum elastic strain equals to 0.00386. Fig. 9 shows the IEA curves for different loading conditions, i.e., stand-off distances and depth parameters listed in Table 1, for Plate 10 (a, b) and Plate 18 (c, d). By looking at IEA curves, it can be deduced that for simple configuration of plates, curves' scatter is more obvious. Depth parameter has a significant impact on damage of plates in near stand-off distances. This effect is deteriorated in farther stand-offs and curves are more dense for medium and far distant loading cases. In near distant explosions, lower charges can produce same overpressures which happen by heavier charges in farther distances. Because initial surrounding pressure induced by depth parameter will affect weaker charges more severely, temporal history of pressure and its effect on structures are more altered and this is a robust justification for such a distribution of IEA curves in which the scattering of curves are more influenced by the depths parameter for near distant stand-offs.

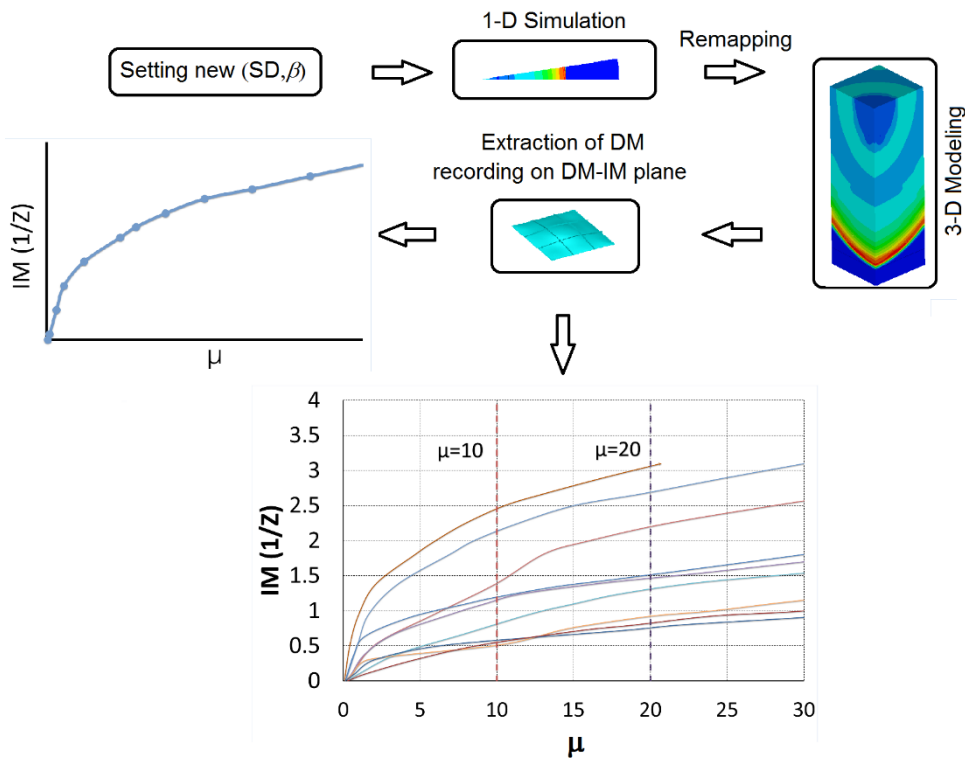


Fig. 6 Schematic representation of Incremental Explosive Analysis (IEA) procedure

Table 7 Incremental values of IMs for different configurations and different standoff distances

Configuration	standoff distance (mm)	$\Delta(\frac{1}{Z})$	Configuration	standoff distance (mm)	$\Delta(\frac{1}{Z})$
Plate 10	700	0.45	Plate 18 – one directiona 1 stiffened	700	0.6
	1400	0.29		1400	0.31
	2100	0.21		2100	0.25
Plate 18	700	0.6	Plate 18 – two directiona 1 stiffened	700	0.65
	1400	0.29		1400	0.33
	2100	0.21		2100	0.25

By reinforcing plates by stiffeners, what is more discernible is the scattering of curves channelization for every stand-off case (Fig. 10). But again rigorous effect of depth on near distant loading cases is observable. For all stand-off parameters UNDEX curves are slightly compressed with respect to those of plates without stiffeners. One of the main effects of depth parameter is the introduction of preloading on plates before shock loading. The increased rigidity due to stiffening of plates reduces preloading deflection and because in farther distances explosions are less affected by depth, curves are less dependent on the depth parameter and the stand-off parameter has more effect on distribution of IEA curves.

In both Fig. 9 and 10, it can be observed that increasing of depth parameter, from 7 to 90, yields lower values of the corresponding IMs which the plate experiences, i.e., reaching to elastic limit state. It can be concluded that the higher values of depth parameter lowers the IM values in a distinct way. This could be inferable that higher hydrostatic pressures can put plates in more perilous situations by means of lower weight of charges. For instance, according to Fig. 10(b), the IM values decrease when the depth parameter increases from 7 to 90 with the same stand-off distance values, i.e. 700, to reach the elastic limit state. A characteristics of IEA curves is that a distinctive part of curves are linear for medium and far distant explosions while for near distant UNDEX, transition from linear to nonlinear regime is gradual. Higher local deformations and strain rate effects in the middle of plates can be a logical justification for this behavior. Nevertheless, it is evident that the higher IMs are required to make the same DM levels in plates due to the significant

effect of rate sensitive plasticity in near distant explosion cases as discussed in Hajjalizadeh [37]. This fact shows that ignoring strain rate effect in the design of blast resistant structures results in overestimations, particularly in near distant explosions, where the performance of the structure may be related to its weight, particularly for moving structures. Since elicitation of IEA curves are greatly influenced by loading conditions and having all these conditions to be accurately taken into account is not practical, there should be further statistical studies to determine the probable damage approximation of structures when facing the similar critical situations. As discussed in section 2.2, in order to show the approximate survival odds of a structure under different adverse conditions, the IEA curves need to be summarized. There are several methods to summarize the IEA curves. In this study, the method of fractiles has been employed based on the maximum edge rotation (θ_{max}) DM parameter to illustrate its usage. This method summarized the results of analysis into their 16%, 50%, and 84% fractile. This means that categorizing of the obtained results into the three different makes it feasible to be aware of the probability of the occurring an identical damage regarded to specific configuration and loading conditions. These three percentiles are chosen based on the normal distribution of obtained values.

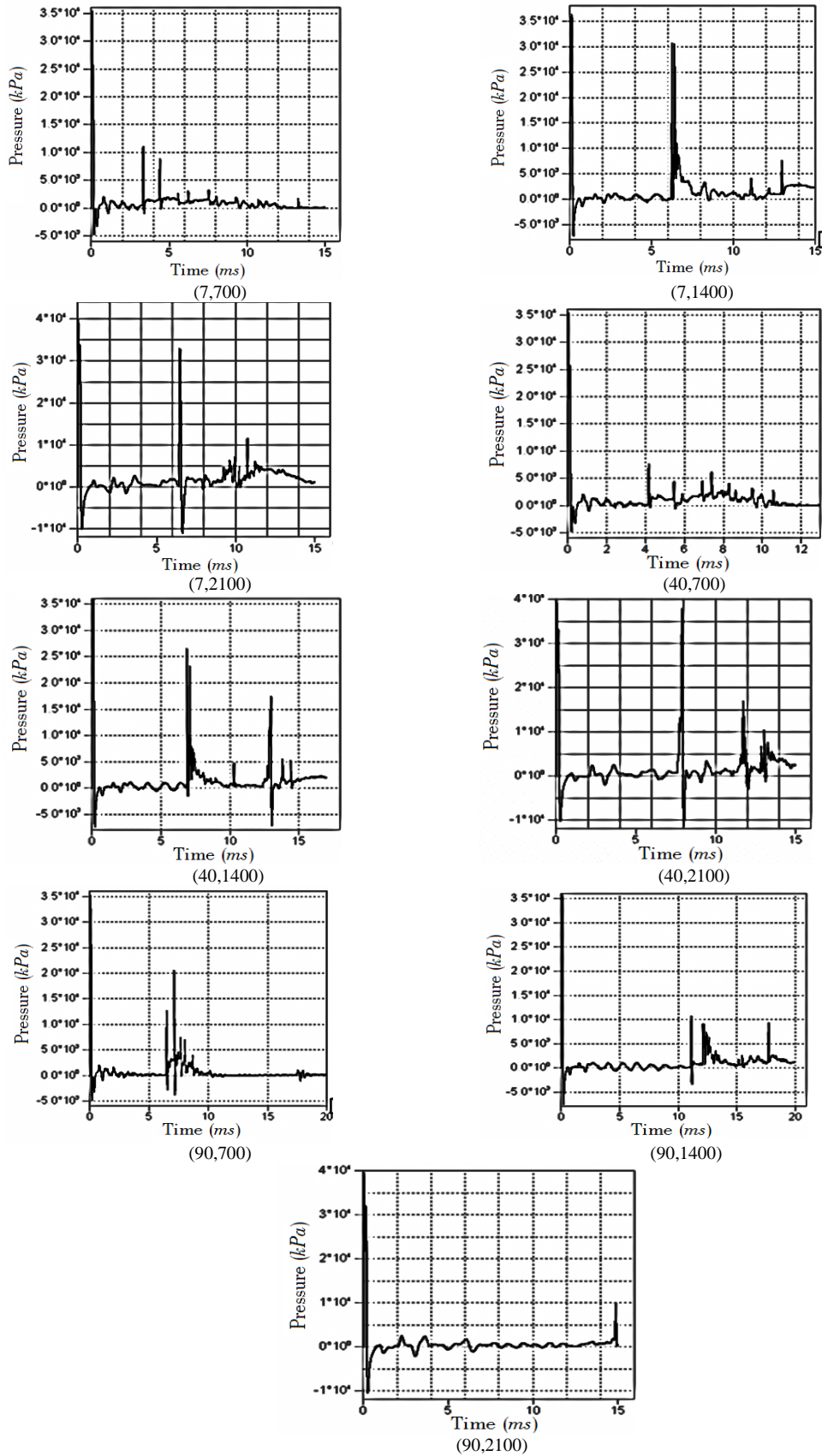


Fig. 7 Pressure time histories for a sample case, $IM=1/Z=0.93$ (kg0.3/m), (β ,SD(mm)).

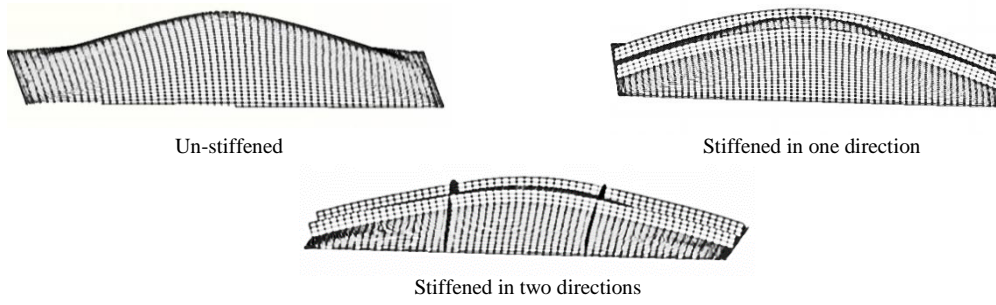


Fig. 8 Deformed configuration of plates at maximum DM.

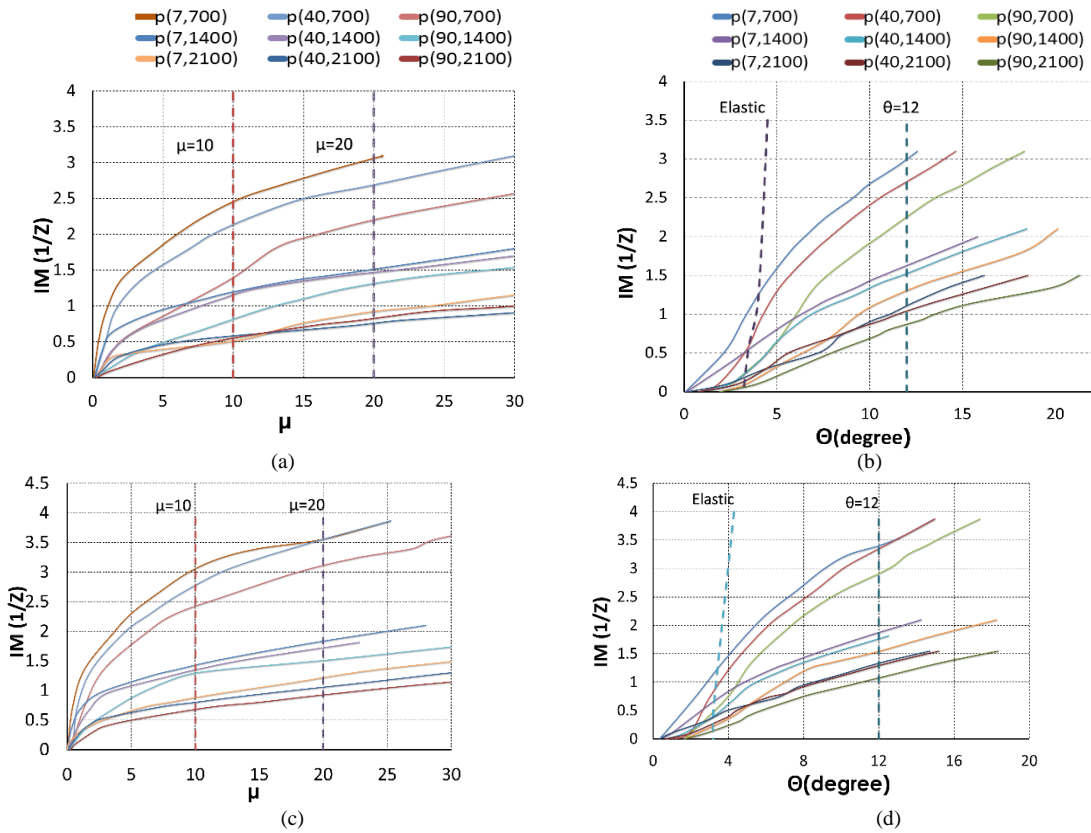


Fig. 9 IEA curves of plate 10 and Plate 18. Plate 10: (a) $1/Z - \mu$ diagram (b) $1/Z - \theta$ diagram. Plate 18: (c) $1/Z - \mu$ diagram (d) $1/Z - \theta$ diagram

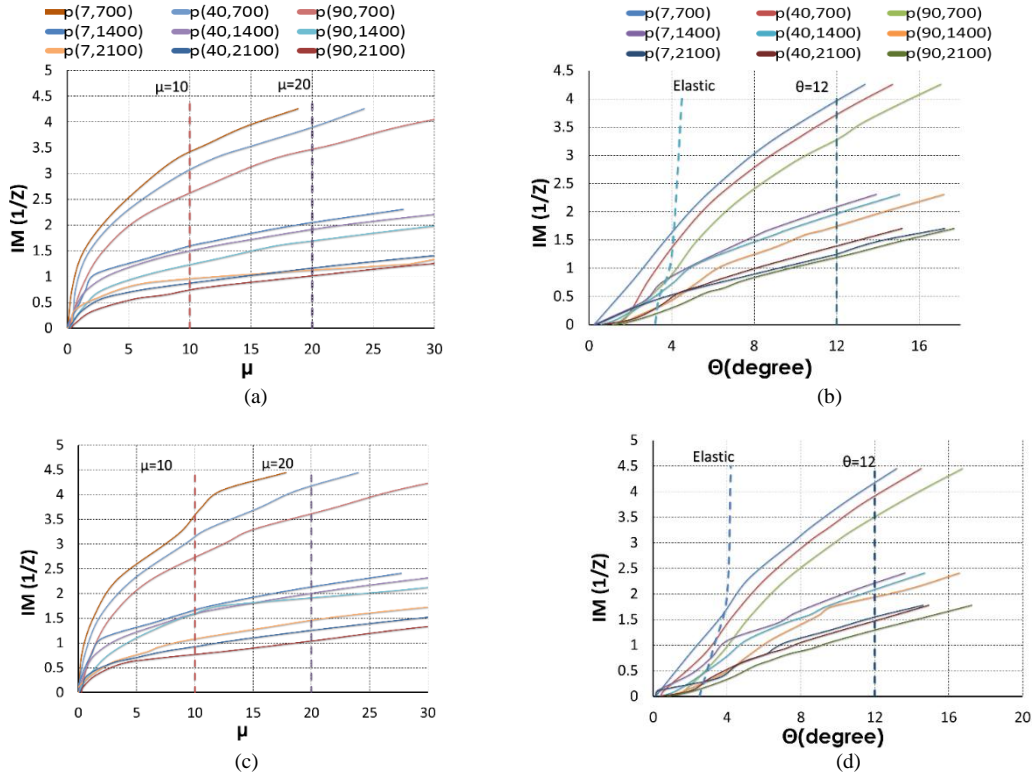


Fig. 10 IEA curves of Plate 18 with stiffeners. Plate 18 with one-direction stiffener: (a) $1/Z - \mu$ diagram, (b) $1/Z - \theta$ diagram. Plate 18 with cross stiffeners: (c) $1/Z - \mu$ diagram, (d) $1/Z - \theta$ diagram

Fig. 11 depicts the IEA curves of the four different plates with these percentiles alongside with corresponding limit-states. According to Fig. 10 (a), for the acquired $IM (1/Z) = 1.0$, 16% of explosions yield $\theta_{max} \leq 3.6^\circ$, 50 % of them result in $\theta_{max} \leq 6.6^\circ$ and 84% of detonations produce $\theta_{max} \leq 12.5^\circ$, approximately. As the thickness of the plate increases, the exact same amount of $1/Z$ values results in smaller values of θ_{max} since the bending stiffness of the plate increases significantly. As it can be seen, by comparing Fig. 11(b) with Fig. 11(a), the elastic limit state has been moved to the left indicating that the elastic limit state will be reached for smaller values of θ_{max} . Furthermore, for the given $IM (1/Z) = 1.0$, 16% of the explosions yield $\theta_{max} \leq 2.2^\circ$, 50 % of them result in $\theta_{max} \leq 5.5^\circ$ and 84% of the detonations produce $\theta_{max} \leq 9.9^\circ$, approximately. As explained earlier, higher values of $1/Z$ results in higher strain rates which leads to higher failure stresses. Comparing Fig. 10(b) with those with stiffener reinforcement (c, d), it is obvious that obtaining a certain value of θ_{max} requires more values of $1/Z$ indicating that the stiffeners have definite role in reinforcing underwater structures facing detrimental effects of possible explosions. According to Fig. 11, in order to achieve $\theta_{max} = 8^\circ$ with considering the fractile of 84%, the $IM (1/Z)$ becomes approximately 0.85 for case (b),

0.93 for case (c) and finally 0.98 for case (d). This can be interpreted as higher amount of explosive is needed to yield a specific damage when the plate was reinforced by one and cross directional stiffeners.

In addition, another useful and more convenient tool for designers who deal with design and assessment of marine structure subjected to loadings with a probability essence is fragility curves Tehrani [22]. After performing preliminary analysis to attain the IEA data for a specific structure, the fragility curves can be used to anticipate if the structure has exceeded certain limit state, e.g., elastic limit state. Considering the fact that the IEA data have normal distributions, it is practical to derive the fragility curves for a specific limit state. In order to obtain these curves for the IEAs provided and discussed earlier, the normal logarithm curve is employed and finally the Error Function or Gauss Error Function is obtained by the following equations [38]:

$$\mu^* = \log\left(\frac{m^{*2}}{\sqrt{v + m^{*2}}}\right) \tag{17}$$

$$\sigma^* = \sqrt{\log(v + m^{*2} + 1)} \tag{18}$$

$$y = f(x, \mu^*, \sigma^*) = \frac{1}{x\sigma^* \sqrt{2\pi}} e^{-\frac{(\ln(x) - \mu^*)^2}{2\sigma^{*2}}} \tag{19}$$

$$Y = \frac{1}{2} + \frac{1}{2} \operatorname{erf} \left[\frac{\ln(x) - \mu^*}{\sigma^* \sqrt{2}} \right] \quad (20)$$

where m^* , v , μ^* and σ^* are the average, the variance, the location parameter and the scale parameter of the IEA data, respectively. The parameter y refers to the probability density function of occurrence x and Y stands for accumulative distribution function which is drawn in Fig. 11.

Fig. 12 shows the fragility analysis conducted on the plates; the probability (percentile) of exceeding the certain limit state with respect to $IM (1/Z)$ value obtained from IEA.

Fig. 12 provides useful information about the possibilities of damage on different operational conditions. For example, for plate 10 (Fig. 12 (a)), the probability of achieving elastic and LS-2 states when experiencing $IM (1/Z) = 1.0$ equals to approximately 90 % and 22 %, respectively. On the other hand, when the Plate 18 is exposed to the same $IM (1/Z)$, this probability reduces to approximately 83 % and 15 %, for emerging of elastic and LS-2 conditions, respectively. By comparing case (b) with the next two cases (c, d), it can be observed that enhancing the strength of the plate results in lower probabilities when a specific $IM (1/Z)$ value is applied to the structure. For instance, for given $IM (1/Z) = 1.0$, the probabilities that the unidirectional and cross direction al stiffened plates reach the elastic state is almost 81% and 78%, respectively, and to exceed the LS-2 state it is approximately 10% for both configurations.

7. Conclusions

In this paper, a relatively novel approach is established for performance-based assessment of stiffened and unstiffened square plates subjected to UNDEX. Since this approach gains its advantages generally from the incremental dynamic analysis, the proposed methodology is called incremental explosive analysis. The performance of structures, which are intended to be explosion resistance, can be evaluated by IEA considering uncertain nature of explosive loading. The both demand and capacity of structures were addressed by IEA. The

rigorous analysis led to produce the multi IEA curves as representing the plates' responses. The statistical treatment of the obtained IEA curves was performed in order to summarize the results and to use them effectively in a predictive mode. The variability and vagaries of a nonlinear structural system under UNDEX loads leads to the need for this treatment. The stand-off distance and depth parameter that influence UNDEX loading and its uncertain character were chosen for this primary study. In addition, the fragility curves were extracted from data that obtained from IEA. The use of IEA approach can be generalized for other fields of blast engineering such as underground and in air explosions by their special considerations.

The most important results of the present study can be outlined as follows:

- By increasing the stand-off distance, distribution of pressure will be more uniform and the effect of depth will be less sensible due to heavier charges which are less affected by initial pressure of the surrounding medium.
- The IEA may use as an applicable method to derive the structural performance in the whole range of elastic and elasto-plastic states of the structure and to demonstrate the structural capacity in a more sensible and comprehensible way.
- Scattering of the IEA curves are more influenced by the depths parameter for near distant stand-offs. It shows that the depth parameter has a significant impact on damage of plates in near stand-off distances. This effect is reduced in farther stand-offs and curves are more dense for medium and far distant loading cases.
- According to IEA curves, increasing of depth parameter yields lower values of the corresponding IMs that plate experiences for reaching specific limit state i.e., elastic limit state. This could be deduced that higher hydrostatic pressures can put plates in more critical situations even with weaker charges.
- Stiffeners are more effective in farther stand-offs due to the global deformation of structure while in nearer stand-offs local loading reduces the effective functioning of stiffeners.
- In far stand-offs a distinguished linear elastic part can be observed on IEA curves while in near distance explosions, due to the higher effect of strain rate, a gradual transition to nonlinear portion of response is more sensible.
- Summarization of IEA curves and constructing the fragility curves results in a concise presentation of data which can assist designers for better judgments and decision makings about performance of structure against various level of UNDEX threats.

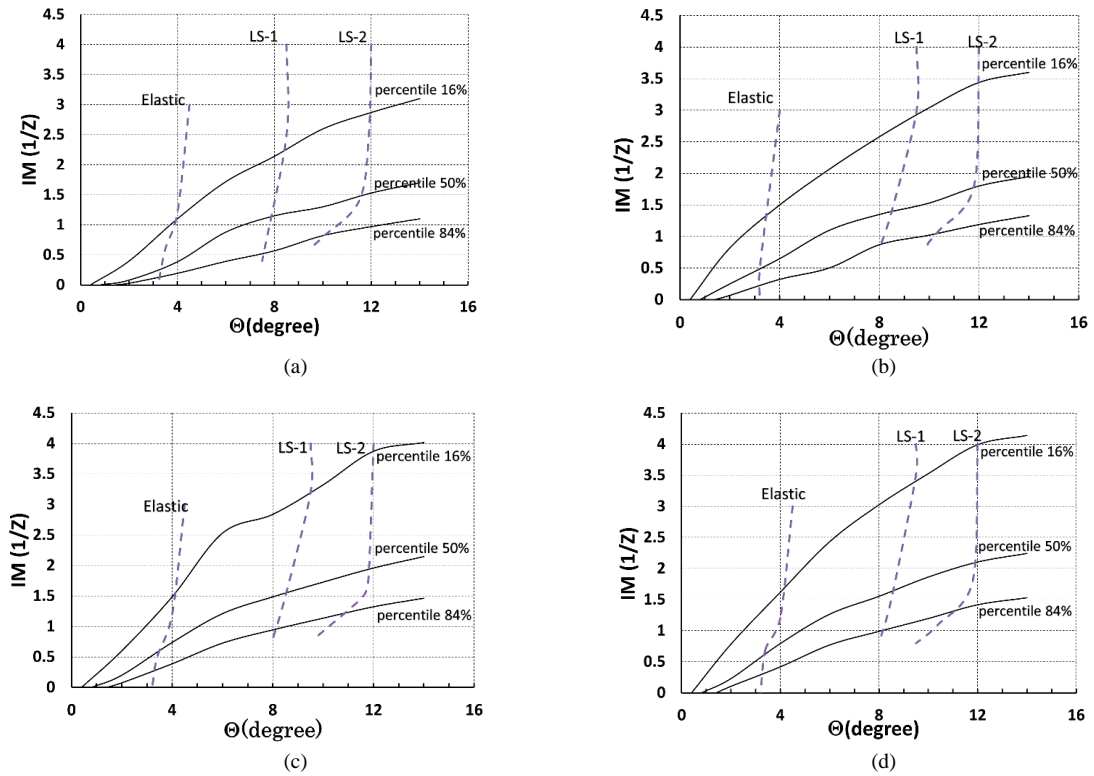


Fig. 11 IEA curves of plates with three percentiles including distinct limit-states; (a) Plate 10, (b) plate 18, (c) Plate 18 with one-directional stiffener and (d) Plate 18 with cross stiffeners

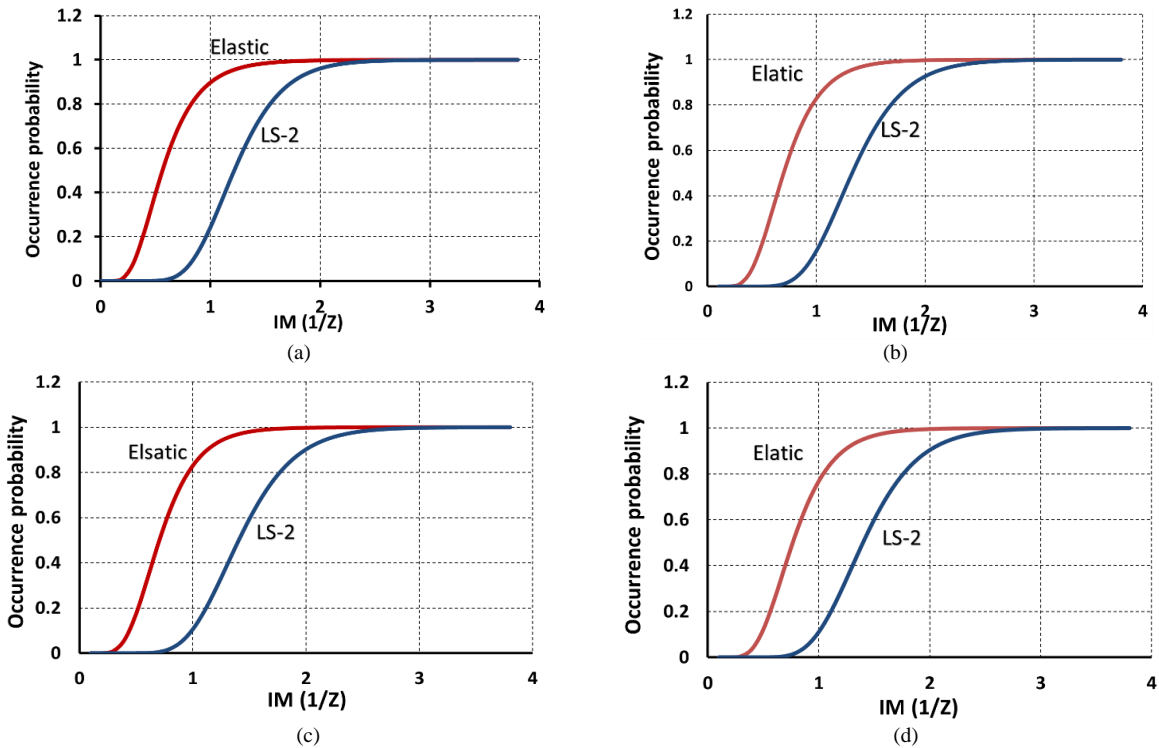


Fig. 12 Fragility curves of plates with distinct limit-states; (a) Plate 10, (b) plate 18, (c) Plate 18 with one-directional stiffener and (d) Plate 18 with cross stiffeners

References

- [1] R. H. Cole, R. Weller, 1948, *Underwater explosions*,
- [2] K. Ramajeyathilagam, C. Vendhan, V. B. Rao, Non-linear transient dynamic response of rectangular plates under shock loading, *International Journal of Impact Engineering*, Vol. 24, No. 10, pp. 999-1015, 2000.
- [3] H. Gharababaei, A. Darvizeh, M. Darvizeh, Analytical and experimental studies for deformation of circular plates subjected to blast loading, *Journal of mechanical Science and Technology*, Vol. 24, No. 9, pp. 1855-1864, 2010.
- [4] A. Bayat, R. Moharami, Numerical Analysis of explosion effects on the redistribution of residual stresses in the underwater welded pipe, *Journal of Computational Applied Mechanics*, Vol. 47, No. 1, pp. 121-128, 2016.
- [5] R. Rajendran, J. Paik, J. Lee, Of underwater explosion experiments on plane plates, *Experimental Techniques*, Vol. 31, No. 1, pp. 18-24, 2007.
- [6] R. Rajendran, K. Narashimhan, Performance evaluation of HSLA steel subjected to underwater explosion, *Journal of Materials Engineering and Performance*, Vol. 10, No. 1, pp. 66-74, 2001.
- [7] C. Hung, P. Hsu, J. Hwang-Fuu, Elastic shock response of an air-backed plate to underwater explosion, *International Journal of Impact Engineering*, Vol. 31, No. 2, pp. 151-168, 2005.
- [8] N. Gupta, P. Kumar, S. Hegde, On deformation and tearing of stiffened and un-stiffened square plates subjected to underwater explosion—a numerical study, *International Journal of Mechanical Sciences*, Vol. 52, No. 5, pp. 733-744, 2010.
- [9] L. Li, W. Jiang, A new effective method to predict the permanent deformation of plane plates subjected to underwater shock loading, *Proceedings of the Institution of Mechanical Engineers, Part C: Journal of Mechanical Engineering Science*, Vol. 225, No. 5, pp. 1069-1075, 2011.
- [10] R. Rajendran, Numerical simulation of response of plane plates subjected to uniform primary shock loading of non-contact underwater explosion, *Materials & Design*, Vol. 30, No. 4, pp. 1000-1007, 2009.
- [11] R. Rajendran, Reloading effects on plane plates subjected to non-contact underwater explosion, *Journal of materials processing technology*, Vol. 206, No. 1, pp. 275-281, 2008.
- [12] P. Ren, W. Zhang, Underwater shock response of air-backed thin aluminum alloy plates: An experimental and numerical study, in *Proceeding of*, IOP Publishing, pp. 182034.
- [13] R. Rajendran, K. Narasimhan, Deformation and fracture behaviour of plate specimens subjected to underwater explosion—a review, *International Journal of Impact Engineering*, Vol. 32, No. 12, pp. 1945-1963, 2006.
- [14] G.-S. Yeom, Numerical study of underwater explosion near a free surface and a structural object on unstructured grid, *Journal of Mechanical Science and Technology*, Vol. 29, No. 10, pp. 4213-4222, 2015.
- [15] M. Grujicic, B. Pandurangan, C. Zhao, B. Cheeseman, A computational investigation of various water-induced explosion mitigation mechanisms, *Multidiscipline Modeling in Materials and Structures*, Vol. 3, No. 2, pp. 185-212, 2007.
- [16] G. Wang, S. Zhang, M. Yu, H. Li, Y. Kong, Investigation of the shock wave propagation characteristics and cavitation effects of underwater explosion near boundaries, *Applied Ocean Research*, Vol. 46, pp. 40-53, 2014.
- [17] D. Vamvatsikos, C. A. Cornell, Incremental dynamic analysis, *Earthquake Engineering & Structural Dynamics*, Vol. 31, No. 3, pp. 491-514, 2002.
- [18] D. Vamvatsikos, C. A. Cornell, The incremental dynamic analysis and its application to performance-based earthquake engineering, in *Proceeding of*, Citeseer, pp.
- [19] D. Vamvatsikos, C. A. Cornell, Applied incremental dynamic analysis, *Earthquake Spectra*, Vol. 20, No. 2, pp.

- 523-553, 2004.
- [20] A. Zacharenaki, M. Fragiadakis, D. Assimaki, M. Papadrakakis, Bias assessment in Incremental Dynamic Analysis due to record scaling, *Soil Dynamics and Earthquake Engineering*, Vol. 67, pp. 158-168, 2014.
- [21] M. Alembagheri, M. Ghaemian, Damage assessment of a concrete arch dam through nonlinear incremental dynamic analysis, *Soil Dynamics and Earthquake Engineering*, Vol. 44, pp. 127-137, 2013.
- [22] P. Tehrani, D. Mitchell, Seismic performance assessment of bridges in Montreal using incremental dynamic analysis, in *Proceeding of*.
- [23] A. Ajamy, M. Zolfaghari, B. Asgarian, C. Ventura, Probabilistic seismic analysis of offshore platforms incorporating uncertainty in soil–pile–structure interactions, *Journal of Constructional Steel Research*, Vol. 101, pp. 265-279, 2014.
- [24] B. Asgarian, A. Ajamy, Seismic performance of jacket type offshore platforms through incremental dynamic analysis, *Journal of Offshore Mechanics and Arctic Engineering*, Vol. 132, No. 3, pp. 031301, 2010.
- [25] M. Zolfaghari, A. Ajamy, B. Asgarian, A simplified method in comparison with comprehensive interaction incremental dynamic analysis to assess seismic performance of jacket-type offshore platforms, *International Journal of Advanced Structural Engineering (IJASE)*, Vol. 7, No. 4, pp. 353-364, 2015.
- [26] A. Golafshani, V. Bagheri, H. Ebrahimian, T. Holmas, Incremental wave analysis and its application to performance-based assessment of jacket platforms, *Journal of Constructional Steel Research*, Vol. 67, No. 10, pp. 1649-1657, 2011.
- [27] M. Zeinoddini, H. M. Nikoo, H. Estekanchi, Endurance Wave Analysis (EWA) and its application for assessment of offshore structures under extreme waves, *Applied Ocean Research*, Vol. 37, pp. 98-110, 2012.
- [28] K. Wei, S. R. Arwade, A. T. Myers, Incremental wind-wave analysis of the structural capacity of offshore wind turbine support structures under extreme loading, *Engineering Structures*, Vol. 79, pp. 58-69, 2014.
- [29] R. A. Izadifard, M. R. Maheri, Application of displacement-based design method to assess the level of structural damage due to blast loads, *Journal of mechanical science and technology*, Vol. 24, No. 3, pp. 649-655, 2010.
- [30] B. Le Méhauté, S. Wang, 1996, *Water waves generated by underwater explosion*, World Scientific,
- [31] U. Army, U. Navy, U. A. Force, Structures to resist the effects of accidental explosions, *TM5-1300*, pp. 1400, 1990.
- [32] G. Farin, 2014, *Curves and surfaces for computer-aided geometric design: a practical guide*, Elsevier,
- [33] E. T. Lee, Choosing nodes in parametric curve interpolation, *Computer-Aided Design*, Vol. 21, No. 6, pp. 363-370, 1989.
- [34] H. Huang, Transient interaction of plane acoustic waves with a spherical elastic shell, *The Journal of the Acoustical Society of America*, Vol. 45, No. 3, pp. 661-670, 1969.
- [35] H. Huang, An exact analysis of the transient interaction of acoustic plane waves with a cylindrical elastic shell, *Journal of Applied Mechanics*, Vol. 37, No. 4, pp. 1091-1099, 1970.
- [36] T. AUTODYN, Theory Manual Revision 4.3, Concord, CA: Century Dynamics, Inc, 2003.
- [37] F. Hajjalizadeh, M. M. Mashhadi, Investigation and numerical analysis of impulsive hydroforming of aluminum 6061-T6 tube, *Journal of Manufacturing Processes*, Vol. 20, pp. 257-273, 2015.
- [38] W. Feller, 2008, *An introduction to probability theory and its applications*, John Wiley & Sons,